PERGAMON

International Journal of Solids and Structures 38 (2001) 3813–3830

INTERNATIONAL JOURNAL OF SOLIDS and STRUCTURES

www.elsevier.com/locate/ijsolstr

Fracture mechanics for a Mode I crack in piezoelectric materials

Fuqian Yang *

Department of Mechanical Engineering, University of Rochester, 233 Hopeman Building, Rochester, NY 14627-0132, USA

Received 13 October 1999; in revised form 21 May 2000

Abstract

Using linear piezoelectricity theory, the effect of a Griffith crack on stress and electric fields in an infinite piezoelectric material under electric and tension loading has been studied by using appropriate boundary conditions. A closed-form solution to the Mode I fracture problem is obtained for external loading used to open the crack. By including electrostatic energy in the calculation of crack driving force, the energy release rate is found to be the third power function of the external loading if electric field inside the crack is not zero at the crack tip. The results may be used to explain some nonlinear phenomenon observed in the indentation of piezoelectric ceramics. © 2001 Elsevier Science Ltd. All rights reserved.

Keywords: Crack; Piezoelectric; Energy release rate; Nonlinear behavior

1. Introduction

Smart structures using smart materials have potential applications in many areas, especially in controlling motion that is related to structural deformation. In these smart materials, piezoelectric materials, shape memory alloys, electrostrictive materials, and magnetostrictive materials have been widely used in electromechanical actuators and sensors. The coupling between mechanical and electric fields in piezoelectric materials provides a mechanism for sensing mechanical disturbances from the measurements of induced electric potentials, and for altering structural responses via external electric fields. Among the piezoelectric materials, piezoelectric ceramics are widely used due to their high piezoelectric performance. However, piezoelectric ceramics in mechanical behavior are brittle and susceptible to cracking at all scales

* Tel.: +1-716-275-8394; fax: +1-716-256-2509.
E-mail address: fuyang@me.rochester.edu (F. Yang).

0020-7683/01/$ - see front matter
PII: S0020-7683(00)00244-4

from microdomains to macrodevices. When a ceramic is poled by an electrostatic field of the order of MV/m, cracks nucleate to relax the incompatible strains (Chung et al., 1989). Many static and cyclic failure of devices have been described by Winzer et al. (1989).

The structural reliability of piezoelectric materials has drawn more and more attention as they are used in microelectromechanical systems. The study of damage and fracture processes in piezoelectric ceramics can provide better understanding of the mechanisms of piezoelectric cracking in the presence of defects such as cracks and improve the device performance to increase system reliability. This has motivated the investigations of fracture mechanics of piezoelectric materials (Parton, 1976; Pak, 1990; Deeg, 1990; Shindo et al., 1990; Kuo and Barnett, 1991; Suo et al., 1992; Dunn, 1994; Zhang and Tong, 1996; Makino and Kmiya, 1994; Cao and Evans, 1994; Yang and Suo, 1994; Gao et al., 1997; Yang and Kao, 1999; Park and Sun, 1995; Li et al., 1990; Kumar and Singh, 1995), and many important achievements have been made over the course of many years. For a crack being treated as a mathematical slit without any thickness and having a finite dielectric constant, there are two commonly used electric boundary conditions along the crack faces. Parton (1976) modeled a crack as a traction free, but permeable slit, that is, the potential and the normal component of the electric displacement are continuous across the crack,

$$\phi^+ = \phi^- \quad \text{and} \quad D_n^+ = D_n^-.$$

Deeg (1980) and Pak (1990) proposed another set of boundary conditions in the crack faces,

$$D_n^+ = D_n^- = 0,$$

which is based on two assumptions: (1) no external free charges in either crack faces, and (2) the electric displacement in the crack is negligible. Based on the electric boundary conditions, Pak (1990) studied a crack with its front coincident with the poling axis. Sosa and Pak (1990) analyzed a more general crack-tip field by using an eigenfunction analysis. Shindo et al. (1990) investigated cracks in piezoelectric layers using integral transforms. Kuo and Barnett (1991) carried out an asymptotic tip analysis. Pak (1990) and Suo et al. (1992) reanalyzed the stress and electric fields near a finite crack. Dunn (1994) studied the effects of crack face boundary conditions on the fracture mechanics of piezoelectric solids. Pak and Tobin (1993) studied the electric boundary conditions in crack faces for piezoelectric materials. They found that crack and the electric field at crack tip had multiple values under different limiting processes.

Recently, the use of the classical electric boundary conditions along the interface of dielectric materials (the continuity of the normal component of electric displacement and tangential component of electric field) in the fracture mechanics of piezoelectric materials has been suggested by Zhang and Hack (1992); Zhang et al. (1996); Zhang (1994). Zhang et al. (1996) studied the effects of the boundary conditions by investigating an elliptical cylinder cavity under antiplane loading. In the limiting condition, they found that the two commonly used boundary conditions are the two extremes of the classical electric boundary conditions and they were able to determine the electric field within the cavity (crack).

Ferroelectric ceramics are known to exhibit nonlinear and hysteresis behavior at large external loading (Jona and Shirane, 1993). Cao and Evans (1994) found the nonlinear mechanical behavior of poled PZT piezoelectrics. Some of the nonlinear behavior of piezoelectric ceramics have been studied by Yang and Suo (1994), Lynch et al. (1995), Hao et al. (1996), and Gao et al. (1997). The application of linear piezoelectric theory would be valid if only a small-scale yield is assumed (Gao et al. 1997). However, the linear piezoelectric fracture mechanics plays an important role in understanding the brittle fracture behavior in piezoelectric ceramics. It will pave a pace for further studying the effect of microscale yielding on fracture behavior of piezoelectric ceramics.

It is the purpose of this work to study the opening mode cracking under general mechanical and uniform electric loading by using the classic electric boundary conditions. The Fourier transforms are used to reduce

the problem to a solution of dual integral equations. Four different general solutions dependent on the material constants are given. In addition, the energy release rate is given in a closed form.

2. Electromechanical equations

Consider a linear piezoelectric material, the governing equations in the Cartesian coordinates $x_i (i = 1, 2, 3)$ are given by

$$\sigma_{ij,i} = 0 \quad \text{and} \quad D_{i,i} = 0, \tag{1}$$

where σ_{ij} is the stress tensor, D_i is the electric displacement vector, the comma denotes partial differentiation with respect to the coordinate x_i, and the Einstein summation convention over repeated indices is used. For an anisotropic piezoelectric material, the constitutive relation is

$$\sigma_{ij} = c_{ijkl}\varepsilon_{kl} - e_{kij}E_k, \quad \text{and} \quad D_i = e_{ikl}\varepsilon_{kl} + \epsilon_{ik}E_k, \tag{2}$$

where ε_{kl} is the strain tensor, E_i is the electric field intensity, c_{ijkl} is the elastic stiffness tensor measured in a constant electric field intensity, e_{ikl} is the piezoelectric tensor measured in possession of a spontaneous electric field, and ϵ_{ik} is the dielectric tensor. Crystal symmetry places restrictions among the components of any tensor that characterizes the material properties of a crystal. The interchange symmetry of the tensors are

$$c_{ijkl} = c_{ijlk} = c_{jikl} = c_{jilk} = c_{klij}, \qquad e_{kij} = e_{kji} \quad \text{and} \quad \epsilon_{ij} = \epsilon_{ji}. \tag{3}$$

The relation between the strain tensor and the displacement, u_i, is given by

$$\varepsilon_{ij} = \frac{1}{2}(u_{i,j} + u_{j,i}), \tag{4}$$

and the electric field intensity is

$$E_i = -\phi_{,i}, \tag{5}$$

where ϕ is the electric potential.

Inside the crack filled with air, the electric potential satisfies the following equation

$$\phi^a_{,ii} = 0 \tag{6}$$

with $D^a_i = \epsilon_0 E^a_i$, the relation between the electric displacement and the electric field intensity, where ϵ_0 is the permittivity of vacuum. Here, the superscript 'a' represents the field variables inside the crack.

It is known that a crystal possessing a center of symmetry cannot be piezoelectric, because no combination of uniform stresses will produce the centers of gravity of the positive and negative charges and produce dipole moment, which is necessary for the production of polarization by stresses (Mason, 1950). Here, we consider only a transversely isotropic piezoelectric material of the hexagonal crystal class 6 mm. The constitutive relations are

$$\begin{pmatrix}\sigma_1\\ \sigma_2\\ \sigma_3\\ \sigma_4\\ \sigma_5\\ \sigma_6\end{pmatrix}=\begin{pmatrix}c_{11} & c_{12} & c_{13} & 0 & 0 & 0\\ c_{12} & c_{11} & c_{13} & 0 & 0 & 0\\ c_{13} & c_{13} & c_{33} & 0 & 0 & 0\\ 0 & 0 & 0 & c_{44} & 0 & 0\\ 0 & 0 & 0 & 0 & c_{44} & 0\\ 0 & 0 & 0 & 0 & 0 & c_{66}\end{pmatrix}\begin{pmatrix}\varepsilon_1\\ \varepsilon_2\\ \varepsilon_3\\ \varepsilon_4\\ \varepsilon_5\\ \varepsilon_6\end{pmatrix}-\begin{pmatrix}0 & 0 & e_{31}\\ 0 & 0 & e_{31}\\ 0 & 0 & e_{33}\\ 0 & e_{15} & 0\\ e_{15} & 0 & 0\\ 0 & 0 & 0\end{pmatrix}\begin{pmatrix}E_1\\ E_2\\ E_3\end{pmatrix},$$

$$\begin{pmatrix}D_1\\ D_2\\ D_3\end{pmatrix}=\begin{pmatrix}0 & 0 & 0 & 0 & e_{15} & 0\\ 0 & 0 & 0 & e_{15} & 0 & 0\\ e_{31} & e_{31} & e_{33} & 0 & 0 & 0\end{pmatrix}\begin{pmatrix}\varepsilon_1\\ \varepsilon_2\\ \varepsilon_3\\ \varepsilon_4\\ \varepsilon_5\\ \varepsilon_6\end{pmatrix}+\begin{pmatrix}\epsilon_{11} & 0 & 0\\ 0 & \epsilon_{11} & 0\\ 0 & 0 & \epsilon_{33}\end{pmatrix}\begin{pmatrix}E_1\\ E_2\\ E_3\end{pmatrix}, \tag{7}$$

where

$$\begin{pmatrix}\sigma_1 & \sigma_2 & \sigma_3 & \sigma_4 & \sigma_5 & \sigma_6\\ \varepsilon_1 & \varepsilon_2 & \varepsilon_3 & \varepsilon_4 & \varepsilon_5 & \varepsilon_6\end{pmatrix}=\begin{pmatrix}\sigma_{11} & \sigma_{22} & \sigma_{33} & \sigma_{23} & \sigma_{13} & \sigma_{12}\\ \varepsilon_{11} & \varepsilon_{22} & \varepsilon_{33} & 2\varepsilon_{23} & 2\varepsilon_{13} & 2\varepsilon_{12}\end{pmatrix},$$
$$c_{11}=c_{1111}=c_{2222},\quad c_{12}=c_{1122},\quad c_{13}=c_{1133}=c_{2233},\quad c_{33}=c_{3333},\quad c_{44}=c_{2323}=c_{3131},$$
$$c_{66}=c_{1212}=\tfrac{1}{2}(c_{11}-c_{22}),\quad e_{31}=e_{311}=e_{322},\quad e_{33}=e_{333},\quad e_{15}=e_{113}=e_{223}. \tag{8}$$

3. General solution of two-dimensional piezoelectric coupling problems

For two-dimensional piezoelectric coupling problems in plane strain, the governing equations become

$$\begin{aligned}&c_{11}\frac{\partial^2 u_1}{\partial x_1^2}+c_{44}\frac{\partial^2 u_1}{\partial x_3^2}+(c_{13}+c_{44})\frac{\partial^2 u_3}{\partial x_1\partial x_3}+(e_{31}+e_{15})\frac{\partial^2\phi}{\partial x_1\partial x_3}=0,\\ &(c_{13}+c_{44})\frac{\partial^2 u_1}{\partial x_1\partial x_3}+c_{44}\frac{\partial^2 u_3}{\partial x_1^2}+c_{33}\frac{\partial^2 u_3}{\partial x_3^2}+e_{15}\frac{\partial^2\phi}{\partial x_1^2}+e_{33}\frac{\partial^2\phi}{\partial x_3^2}=0,\\ &(e_{31}+e_{15})\frac{\partial^2 u_1}{\partial x_1\partial x_3}+e_{15}\frac{\partial^2 u_3}{\partial x_1^2}+e_{33}\frac{\partial^2 u_3}{\partial x_3^2}-\epsilon_{11}\frac{\partial^2\phi}{\partial x_1^2}-\epsilon_{33}\frac{\partial^2\phi}{\partial x_3^2}=0,\end{aligned} \tag{9}$$

which can be expressed as

$$[D]\begin{pmatrix}u_1\\ u_3\\ \phi\end{pmatrix}=0, \tag{10}$$

where the operator is

$$[D]=\begin{pmatrix}c_{11}\frac{\partial^2}{\partial x_1^2}+c_{44}\frac{\partial^2}{\partial x_3^2} & (c_{13}+c_{44})\frac{\partial^2}{\partial x_1\partial x_3} & (e_{31}+e_{15})\frac{\partial^2}{\partial x_1\partial x_3}\\ (c_{13}+c_{44})\frac{\partial^2}{\partial x_1\partial x_3} & c_{44}\frac{\partial^2}{\partial x_1^2}+c_{33}\frac{\partial^2}{\partial x_3^2} & e_{15}\frac{\partial^2}{\partial x_1^2}+e_{33}\frac{\partial^2}{\partial x_3^2}\\ (e_{31}+e_{15})\frac{\partial^2}{\partial x_1\partial x_3} & e_{15}\frac{\partial^2}{\partial x_1^2}+e_{33}\frac{\partial^2}{\partial x_3^2} & -(\epsilon_{11}\frac{\partial^2}{\partial x_1^2}+\epsilon_{33}\frac{\partial^2}{\partial x_3^2})\end{pmatrix}. \tag{11}$$

The determinant of $[D]$ is

$$\det[D] = a\frac{\partial^6}{\partial x_3^6} + b\frac{\partial^6}{\partial x_3^4 \partial x_1^2} + c\frac{\partial^6}{\partial x_3^2 \partial x_1^4} + d\frac{\partial^6}{\partial x_1^6} \tag{12}$$

in which

$$\begin{aligned}
a &= -c_{44}\left(e_{33}^2 + c_{33}\epsilon_{33}\right),\\
b &= \Big[2e_{33}c_{13}(e_{31}+e_{15}) + \epsilon_{33}(c_{13}+c_{44})^2 - c_{11}\left(e_{33}^2 + c_{33}\epsilon_{33}\right) - c_{44}(c_{33}\epsilon_{11} + c_{44}\epsilon_{33} - 2e_{33}e_{31})\\
&\quad - c_{33}(e_{31}+e_{15})^2\Big],\\
c &= \Big[2e_{15}(e_{31}+e_{15})(c_{13}+c_{44}) + \epsilon_{11}(c_{13}+c_{44})^2 - c_{11}(c_{44}\epsilon_{33} + c_{33}\epsilon_{11} + 2e_{33}e_{15})\\
&\quad - c_{44}\Big[e_{15}^2 + c_{44}\epsilon_{11} + (e_{31}+e_{15})^2\Big]\Big],\\
d &= -c_{11}\left(e_{15}^2 + c_{44}\epsilon_{11}\right).
\end{aligned} \tag{13}$$

Based on the cofactors Δ_{ij} of $\det[D]$ $(i,j=1,2,3)$, and the method developed by Ding et al. (1996), the general solutions of Eq. (12) are

$$(u_1, u_3, \phi)^{\mathrm{T}} = (\Delta_{i1}, \Delta_{i2}, \Delta_{i3})^{\mathrm{T}} F \qquad (i=1,2,3) \tag{14}$$

with F satisfying the equation

$$\det[D]F = 0. \tag{15}$$

In the following analysis, we use only $(\Delta_{21}, \Delta_{22}, \Delta_{23})$ for problems symmetric about the x_3-axis

$$\begin{aligned}
\Delta_{21} &= \alpha_1 \frac{\partial^4}{\partial x_1^3 \partial x_3} + \alpha_2 \frac{\partial^4}{\partial x_1 \partial x_3^3},\\
\Delta_{22} &= -c_{11}\epsilon_{11}\frac{\partial^4}{\partial x_1^4} - \alpha_3 \frac{\partial^4}{\partial x_1^2 \partial x_3^2} - c_{44}\epsilon_{33}\frac{\partial^4}{\partial x_3^4},\\
\Delta_{23} &= -c_{11}e_{15}\frac{\partial^4}{\partial x_1^4} - \alpha_4 \frac{\partial^4}{\partial x_1^2 \partial x_3^2} - c_{44}e_{33}\frac{\partial^4}{\partial x_3^4},
\end{aligned} \tag{16}$$

where

$$\begin{pmatrix} \alpha_1 \\ \alpha_2 \\ \alpha_3 \\ \alpha_4 \end{pmatrix} = \begin{pmatrix} (c_{13}+c_{44})\epsilon_{11} + (e_{15}+e_{31})e_{15} \\ (c_{13}+c_{44})\epsilon_{33} + (e_{15}+e_{31})e_{33} \\ c_{11}\epsilon_{33} + c_{44}\epsilon_{11} + (e_{15}+e_{31})^2 \\ c_{13}e_{33} - c_{13}(e_{15}+e_{31}) - c_{44}e_{31} \end{pmatrix}. \tag{17}$$

Using the symmetry on x_3-axis and the Fourier transform on x_1, F can be expressed as

$$F = \frac{2}{\pi}\int_0^\infty f(\xi, x_3)\cos(x_1\xi)\mathrm{d}\xi. \tag{18}$$

Substitution of Eq. (18) into Eq. (15) yields

$$a\frac{\mathrm{d}^6 f}{\mathrm{d}x_3^6} - b\xi^2\frac{\mathrm{d}^4 f}{\mathrm{d}x_3^4} + c\xi^4\frac{\mathrm{d}^2 f}{\mathrm{d}x_3^2} - d\xi^6 = 0, \tag{19}$$

which is a homogeneous equation. The solution of f is a function of $\exp(\lambda\xi x_3)$ in which λ is the root of the algebraic equation

$$a\lambda^6 - b\lambda^4 + c\lambda^2 - d = 0. \tag{20}$$

Let $\tilde{\lambda}^2 = \lambda^2 + b/3a$. Then, Eq. (20) becomes

$$\tilde{\lambda}^6 + p\tilde{\lambda}^2 + q = 0 \tag{21}$$

with

$$p = \frac{7b^2}{3a^2} + \frac{c}{a} \quad \text{and} \quad q = \frac{bc}{3a^2} - \frac{d}{a} - \frac{2b^3}{27a^3} \tag{22}$$

whose roots ($\tilde{\lambda}^2$) are

$$\begin{aligned}
\tilde{\lambda}_1^2 &= \sqrt[3]{-\frac{q}{2} + \sqrt{\left(\frac{q}{2}\right)^2 + \left(\frac{p}{3}\right)^3}} + \sqrt[3]{-\frac{q}{2} - \sqrt{\left(\frac{q}{2}\right)^2 + \left(\frac{p}{3}\right)^3}}, \\
\tilde{\lambda}_2^2 &= \omega\sqrt[3]{-\frac{q}{2} + \sqrt{\left(\frac{q}{2}\right)^2 + \left(\frac{p}{3}\right)^3}} + \omega^2\sqrt[3]{-\frac{q}{2} - \sqrt{\left(\frac{q}{2}\right)^2 + \left(\frac{p}{3}\right)^3}}, \\
\tilde{\lambda}_3^2 &= \omega^2\sqrt[3]{-\frac{q}{2} + \sqrt{\left(\frac{q}{2}\right)^2 + \left(\frac{p}{3}\right)^3}} + \omega\sqrt[3]{-\frac{q}{2} - \sqrt{\left(\frac{q}{2}\right)^2 + \left(\frac{p}{3}\right)^3}},
\end{aligned} \tag{23}$$

where $\omega = (-1 + \mathrm{i}\sqrt{3})/2$. The properties of the roots $\tilde{\lambda}^2$ depends on the parameter, $\Delta = q^2/4 + p^3/27$: (1) $\Delta > 0$, one real root and a pair of conjugate complex roots, (2) $\Delta = 0$, three real roots, (a) $p = q = 0$, $\tilde{\lambda}_1^2 = \tilde{\lambda}_2^2 = \tilde{\lambda}_3^2 = 0$, (b) $q^2/4 = -p^3/27 \neq 0$, $\tilde{\lambda}_1^2 \neq \tilde{\lambda}_2^2 = \tilde{\lambda}_3^2$, and (3) $\Delta < 0$, three real roots, $\tilde{\lambda}_1^2 \neq \tilde{\lambda}_2^2 \neq \tilde{\lambda}_3^2$. Based on Eqs. (13) and (20), we obtain

$$\lambda_1^2\lambda_2^2\lambda_3^2 = \frac{c_{11}(e_{15}^2 + c_{44}\epsilon_{11})}{c_{44}(e_{33}^2 + c_{33}\epsilon_{33})} > 0, \tag{24}$$

which indicates that at least one of the roots $\lambda_i^2 (i = 1, 2, 3)$ is positive.

Here, consider only the upper plane ($x_3 > 0$), under which the fields approach constant values as $x_3 \to \infty$. Depending on the properties of λ^2, the function f has four different general solutions:

(a) If $\lambda_1^2 \neq \lambda_2^2 \neq \lambda_3^2 > 0$, then

$$f = \beta_1 \mathrm{e}^{-\lambda_1\xi x_3} + \beta_2 \mathrm{e}^{-\lambda_2\xi x_3} + \beta_3 \mathrm{e}^{-\lambda_3\xi x_3}, \tag{25}$$

(b) If $\lambda_1^2 \neq \lambda_2^2 = \lambda_3^2 > 0$, then

$$f = \beta_1 \mathrm{e}^{-\lambda_1\xi x_3} + \beta_2 \mathrm{e}^{-\lambda_2\xi x_3} + \beta_3 \xi x_3 \mathrm{e}^{-\lambda_2\xi x_3}, \tag{26}$$

(c) If $\lambda_1^2 = \lambda_2^2 = \lambda_3^2 > 0$, then

$$f = \beta_1 \mathrm{e}^{-\lambda_1\xi x_3} + \beta_2 \xi x_3 \mathrm{e}^{-\lambda_1\xi x_3} + \beta_3 \xi^2 x_3^2 \mathrm{e}^{-\lambda_1\xi x_3}, \tag{27}$$

(d) If $\lambda_1^2 > 0$ and $\lambda_2^2, \lambda_3^2 < 0$ or λ_2^2 and λ_3^2 being a pair of conjugate complex roots, then, in this case, the λ_2 and λ_3 are a pair of conjugate complexes $-\delta \pm \mathrm{i}\omega$. The solution of f is

$$f = \beta_1 \mathrm{e}^{-\lambda_1\xi x_3} + \beta_2 \mathrm{e}^{-\delta\xi x_3} \cos\omega\xi x_3 + \beta_3 \mathrm{e}^{-\delta\xi x_3} \sin\omega\xi x_3, \tag{28}$$

where δ and $\omega > 0$ and β_i $(i = 1, 2, 3)$ is a function of ξ to be determined by the boundary conditions.

Using Eqs. (25)–(28) and Eqs. (14) and (16), the displacement, stress, electric and potential fields for the problems symmetric about the x_3-axis can be readily obtained and briefly given in Appendix A.

4. Opening mode internal crack problems

Consider a finite crack of length $2a_0$ embedded in an infinite piezoelectric medium subjected to electric and mechanical loading as shown in Fig. 1. Due to the linearity of the governing equations and the constitutive relations, we will consider only two different external loading. The first one is a pure mechanical loading applied to the crack faces without external electric field. The second considers a uniform electric field applied at infinity without external mechanical loading, which can be easily implemented in the laboratory.

The electric boundary conditions along the interface between the piezoelectric medium and the dielectric medium for the upper crack face are

$$E_1(x_1,0^+) = E_1^a(x_1,0^-) \quad \text{and} \quad D_3(x_1,0^+) = D_3^a(x_1,0^-) \quad \text{for } |x_1| < a_0, \tag{29}$$

which is identical to

$$\phi(x_1,0^+) = \phi^a(x_1,0^-) \quad \text{and} \quad D_3(x_1,0^+) = D_3^a(x_1,0^-) \quad \text{for } |x_1| < a_0. \tag{30}$$

Similarly, we can have the electric boundary conditions for the lower crack face. The shear stress is

$$\sigma_{13}(x_1,0) = 0. \tag{31}$$

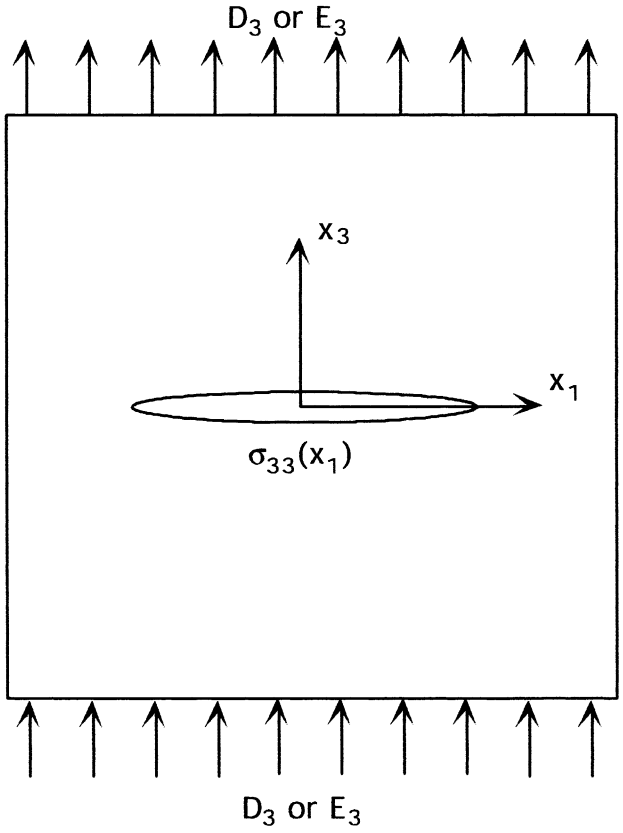

Fig. 1. A Griffith crack in an infinite piezoelectric material.

Due to the symmetry, the displacement and electric potential at the plane $x_3 = 0$ satisfy

$$u_3(x_1, 0) = 0 \quad \text{and} \quad \phi(x_1, 0) = 0 \quad \text{for } |x_1| > a_0. \tag{32}$$

4.1. Mechanical loading on the crack faces in the absence of electric field

In this section, we consider the case that the mechanical loading is applied to the crack faces without external electric field. The other boundary conditions are

$$\sigma_{33} = 0, \quad E_3 = 0 \quad \text{as } x_3 \to \infty, \tag{33}$$

$$\sigma_{33}(x_1, 0) = \sigma_0(x_1) \quad \text{for } |x_1| < a_0. \tag{34}$$

Due to the symmetry, the solution of Eq. (6) can be expressed as

$$\phi^a = \operatorname{sgn}(x_3) \sum_0^\infty \tilde{\beta}_n \sinh\left(\frac{2n+1}{2a_0} x_3\right) \cos\left(\frac{2n+1}{2a_0} x_1\right) \quad \text{inside the crack } (|x_1| < a_0), \tag{35}$$

where $\tilde{\beta}_n (n = 1, 2, 3, \ldots)$ are constants to be determined.

Using the boundary conditions (30)–(34), the field distributions given in Appendix A and Eq. (35), we have the following cases:

(i) for the shear stress

$$b_{11}\beta_1 + b_{12}\beta_2 + b_{13}\beta_3 = 0, \tag{36}$$

(ii) for the electric potential

$$b_{21}\beta_1 + b_{22}\beta_2 + b_{23}\beta_3 = 0, \tag{37}$$

(iii) for the normal stress

$$\frac{2}{\pi} \sum_{i=1}^3 b_{3i} \int_0^\infty \beta_i \xi^5 \cos(\xi x_1) \mathrm{d}\xi = \sigma_0(x_1) \quad \text{for } |x_1| < a_0, \tag{38}$$

(iv) for the displacement

$$\frac{2}{\pi} \sum_{i=1}^3 b_{4i} \int_0^\infty \beta_i \xi^4 \cos(\xi x_1) \mathrm{d}\xi = 0 \quad \text{for } |x_1| > a_0, \tag{39}$$

(v) for the electric displacement

$$\frac{2}{\pi} \sum_{i=1}^3 b_{5i} \int_0^\infty \beta_i \xi^5 \cos(\xi x_1) \mathrm{d}\xi = -\epsilon_0 \sum_0^\infty \tilde{\beta}_n \frac{2n+1}{2a_0} \cos\left(\frac{2n+1}{2a_0} x_1\right) \quad \text{for } |x_1| < a_0, \tag{40}$$

where $b_{ij} (i = 1, 2, 3, 4, 5 \text{ and } j = 1, 2, 3)$ are constants depending on the material properties of piezoelectric materials, which are given in Appendix B.

Eqs. (36) and (37) gives

$$\beta_1 = \frac{\Delta_1}{\Delta} \beta_3 \quad \text{and} \quad \beta_2 = \frac{\Delta_2}{\Delta} \beta_3 \tag{41}$$

with $\Delta = b_{11}b_{22} - b_{12}b_{21}$, $\Delta_1 = b_{12}b_{23} - b_{22}b_{13}$, and $\Delta_2 = b_{12}b_{13} - b_{11}b_{23}$. Substituting Eq. (41) into Eqs. (3) and (39), we obtain

$$\frac{2}{\pi}\left(\frac{\Delta_1}{\Delta}b_{31}+\frac{\Delta_2}{\Delta}b_{32}+b_{33}\right)\int_0^\infty \beta_3\xi^5\cos(\xi x_1)\mathrm{d}\xi=\sigma_0(x_1)\quad \text{for } |x_1|<a_0, \tag{42}$$

$$\int_0^\infty \beta_3\xi^4\cos(\xi x_1)\mathrm{d}\xi=0\quad \text{for } |x_1|>a_0, \tag{43}$$

which are a special case of a pair of dual integral equations (Sneddon, 1951). The complete solution is

$$\beta_3=\sqrt{\frac{\pi}{2}}\xi^{-4}\int_0^{a_0} g(y)J_0(\xi y)\mathrm{d}y, \tag{44}$$

$$g(y)=\sqrt{\frac{2}{\pi}}\left(\frac{\Delta_1}{\Delta}b_{31}+\frac{\Delta_2}{\Delta}b_{32}+b_{33}\right)^{-1} yq(y)\quad \text{and}\quad q(y)=\int_0^y \frac{\sigma_0(x_1)}{\sqrt{y^2-x_1^2}}\mathrm{d}x_1. \tag{45}$$

Using Eqs. (40) and (42), the electric field inside the crack is

$$E_3^a(x_1)=\frac{1}{\epsilon_0}\frac{\Delta_1 b_{51}+\Delta_2 b_{52}+\Delta b_{53}}{\Delta_1 b_{31}+\Delta_2 b_{32}+\Delta b_{33}}\sigma_0(x_1)\quad \text{and}\quad E_1^a(x_1)=0\qquad \text{for } |x_1|<a_0, \tag{46}$$

which has the similar field distribution to the stress applied onto the crack faces. The stress field in front of the crack tip is

$$\sigma_{33}(x_1,0)=\sqrt{\frac{2}{\pi}}\left(\frac{\Delta_1}{\Delta}b_{31}+\frac{\Delta_2}{\Delta}b_{32}+b_{33}\right)\frac{\mathrm{d}}{\mathrm{d}x_1}\int_0^{a_0} g(y)\mathrm{d}y\int_0^\infty J_0(\xi y)\sin(\xi x_1)\mathrm{d}\xi, \tag{47}$$

which can be further simplified as

$$\sigma_{33}(x_1,0)=\sqrt{\frac{2}{\pi}}\left(\frac{\Delta_1}{\Delta}b_{31}+\frac{\Delta_2}{\Delta}b_{32}+b_{33}\right)\frac{\mathrm{d}}{\mathrm{d}x_1}\int_0^{a_0}\frac{g(y)}{\sqrt{x_1^2-y^2}}\mathrm{d}y\quad \text{for } |x_1|>a_0. \tag{48}$$

Eq. (48) can be expressed as follows by substituting Eq. (45), performing integration by parts, and carrying out the differentiation,

$$\sigma_{33}(x_1,0)=-\frac{2}{\pi}\left(\frac{x_1}{\sqrt{x_1^2-a_0^2}}q(a_0)-q(0)-x_1\int_0^{a_0}\frac{q'(t)}{\sqrt{x_1^2-t^2}}\mathrm{d}t\right)\quad \text{for } |x_1|>a_0. \tag{49}$$

The shape of crack, electric field and the electric displacement in front of the crack tip are

$$u_3(x_1,0)=-\frac{2}{\pi}\frac{\Delta_1 b_{41}+\Delta_2 b_{42}+\Delta b_{43}}{\Delta_1 b_{31}+\Delta_2 b_{32}+\Delta b_{33}}\int_{x_1}^{a_0}\frac{tq(t)}{\sqrt{t^2-x_1^2}}\mathrm{d}t\quad \text{for } |x_1|<a_0, \tag{50}$$

$$E_3(x_1,0)=-\frac{2}{\pi}\frac{\Delta_1 b_{e1}+\Delta_2 b_{e2}+\Delta b_{e3}}{\Delta_1 b_{31}+\Delta_2 b_{32}+\Delta b_{33}}\left(\frac{x_1}{\sqrt{x_1^2-a_0^2}}q(a_0)-q(0)-x_1\int_0^{a_0}\frac{q'(t)}{\sqrt{x_1^2-t^2}}\mathrm{d}t\right)\quad \text{for } |x_1|>a_0, \tag{51}$$

$$D_3(x_1,0)=-\frac{2}{\pi}\frac{\Delta_1 b_{51}+\Delta_2 b_{52}+\Delta b_{53}}{\Delta_1 b_{31}+\Delta_2 b_{32}+\Delta b_{33}}\left(\frac{x_1}{\sqrt{x_1^2-a_0^2}}q(a_0)-q(0)-x_1\int_0^{a_0}\frac{q'(t)}{\sqrt{x_1^2-t^2}}\mathrm{d}t\right)\quad \text{for } |x_1|>a_0, \tag{52}$$

and the electric potential is zero at $x_3=0$, where b_{ej} $(j=1,2,3)$ are constants depending on material properties. Eqs. (49), (51) and (52) show that all of the stress field, electric field, and electric displacement

have the square root singularity in front of crack tip. As defined by Pak (1990), the stress intensity factor and electric displacement intensity factor are

$$K_I^\sigma = \lim_{x_1 \to a_0^+} \sqrt{2\pi(x_1 - a_0)}\sigma_{33}(x_1, 0) = -2\sqrt{\frac{a_0}{\pi}} \int_0^{a_0} \frac{\sigma_0(x_1)}{\sqrt{a_0^2 - x_1^2}} \mathrm{d}x_1, \tag{53}$$

$$K_I^D = \frac{\Delta_1 b_{51} + \Delta_2 b_{52} + \Delta b_{53}}{\Delta_1 b_{31} + \Delta_2 b_{32} + \Delta b_{33}} K_I^\sigma. \tag{54}$$

The stress intensity factor is independent of the electromechanical coupling for linear piezoelectric materials under mechanical loading only.

Here, we consider two important cases: (1) a uniform mechanical loading applied onto the crack faces, and (2) a point loading applied in the middle of the crack faces. For a uniform mechanical loading, $\sigma_{33}(x_1, 0) = -\sigma_0$, there are

$$K_I^\sigma = \sqrt{\pi a_0}\sigma_0 \quad \text{and} \quad K_I^D = \frac{\Delta_1 b_{51} + \Delta_2 b_{52} + \Delta b_{53}}{\Delta_1 b_{31} + \Delta_2 b_{32} + \Delta b_{33}} \sqrt{\pi a_0}\sigma_0. \tag{55}$$

For a point loading applied in the middle of the crack faces, we have

$$\sigma_{33}(x_1, 0) = -\sigma_0 \delta(x_1, 0) \quad \text{for } |x_1| < a_0 \tag{56}$$

where $\delta(\ )$ is the delta function. Substituting Eq. (56) into Eqs. (53) and (54), the intensity factors are

$$K_I^\sigma = \sqrt{\frac{a_0}{\pi}}\sigma_0 \quad \text{and} \quad K_I^D = \frac{\Delta_1 b_{51} + \Delta_2 b_{52} + \Delta b_{53}}{\Delta_1 b_{31} + \Delta_2 b_{32} + \Delta b_{33}} \sqrt{\frac{a_0}{\pi}}\sigma_0. \tag{57}$$

4.2. Far field electric loading in the absence of mechanical loading

The important property of piezoelectric materials is the coupling effect between mechanical and electric fields. As discussed in Section 4.1, mechanical loading will generate electric field with field singularity in front of the crack tip. In this section, we analyze the effect of a constant far field electric loading on the deformation of linear piezoelectric materials. There are two different sets of boundary conditions. The first set is

$$\sigma_{33} = 0, \quad E_3 = -E_0 \quad \text{as } x_3 \to \infty, \tag{58}$$

$$\sigma_{33}(x_1, 0) = 0 \quad \text{for } |x_1| < a_0, \tag{59}$$

which corresponds to traction free boundary condition at infinity and the electric field applies tension loading on piezoelectric medium. Using boundary conditions (58), the field distributions inside piezoelectric medium are

$$\phi = E_0 x_3, \qquad u_3 = -\frac{e_{33}}{c_{33}} E_0 x_3, \tag{60}$$

and

$$E^a = -\frac{\epsilon_{33}}{\epsilon_0}\left(1 + \frac{e_{33}^2}{c_{33}\epsilon_{33}}\right) E_0 \tag{61}$$

inside the crack. It is obvious that none of the fields is singular and all the intensity factors are zero.

The second set corresponds to the fixed boundary condition – the strain/displacement of piezoelectric materials at infinity is zero. Eq. (58) becomes

$$\frac{\mathrm{d}u_3}{\mathrm{d}x_3} = 0, \quad E_3 = -E_0 \quad \text{as } x_3 \to \infty. \tag{62}$$

Using Eq. (14), the displacement field and electric potential satisfying Eq. (62) can be expressed as

$$(u_1, u_3, \phi)^{\mathrm{T}} = (\Delta_{i1}, \Delta_{i2}, \Delta_{i3})^{\mathrm{T}} F + (0, 0, E_0 x_3)^{\mathrm{T}}, \tag{63}$$

$$F = \frac{2}{\pi} \int_0^\infty f(\xi, x_3) \cos(x_1 \xi) \mathrm{d}\xi, \tag{64}$$

where $f(\xi, x_3)$ has the same expression as in Eqs. (25)–(28) with $\beta_i (i = 1, 2, 3)$ to be determined. Using boundary conditions and the same procedure as in the above section, we obtain the following equations:

(i) for the shear stress

$$b_{11}\beta_1 + b_{12}\beta_2 + b_{13}\beta_3 = 0, \tag{65}$$

(ii) for the electric potential

$$b_{21}\beta_1 + b_{22}\beta_2 + b_{23}\beta_3 = 0, \tag{66}$$

(iii) for the normal stress

$$\frac{2}{\pi} \sum_{i=1}^{3} b_{3i} \int_0^\infty \beta_i \xi^5 \cos(\xi x_1) \mathrm{d}\xi = -e_{33} E_0 \quad \text{for } |x_1| < a_0, \tag{67}$$

(iv) for the displacement

$$\frac{2}{\pi} \sum_{i=1}^{3} b_{4i} \int_0^\infty \beta_i \xi^4 \cos(\xi x_1) \mathrm{d}\xi = 0 \quad \text{for } |x_1| > a_0, \tag{68}$$

(v) for the electric displacement

$$\frac{2}{\pi} \sum_{i=1}^{3} b_{5i} \int_0^\infty \beta_i \xi^5 \cos(\xi x_1) \mathrm{d}\xi - \epsilon_{33} E_0 = \epsilon_0 E^a \quad \text{for } |x_1| < a_0, \tag{69}$$

where $b_{ij} (i = 1\text{–}5 \text{ and } j = 1\text{–}3)$ are given in Appendix B. The solutions of $\beta_i (i = 1, 2, 3)$ are

$$\beta_3 = -\frac{\pi}{2} \frac{a_0 e_{33} E_0 J_1(\xi a_0)}{\xi^5} \left(\frac{\Delta_1}{\Delta} b_{31} + \frac{\Delta_2}{\Delta} b_{32} + b_{33} \right)^{-1}, \tag{70}$$

$$\beta_1 = \frac{\Delta_1}{\Delta} \beta_3 \quad \text{and} \quad \beta_2 = \frac{\Delta_2}{\Delta} \beta_3$$

with $\Delta = b_{11}b_{22} - b_{12}b_{21}$, $\Delta_1 = b_{12}b_{23} - b_{22}b_{13}$, and $\Delta_2 = b_{12}b_{13} - b_{11}b_{23}$. The electric field inside the crack is

$$E_3^a(x_1) = -\frac{E_0}{\epsilon_0} \left(\frac{\Delta_1 b_{51} + \Delta_2 b_{52} + \Delta b_{53}}{\Delta_1 b_{31} + \Delta_2 b_{32} + \Delta b_{33}} e_{33} + \epsilon_{33} \right) \quad \text{and} \quad E_1^a(x_1) = 0 \quad \text{for } |x_1| < a_0 \tag{71}$$

proportional to the applied field.

The stress component, shape of crack, electric field and the electric displacement in front of the crack tip are

$$\sigma_{33}(x_1, 0) = \frac{x_1 e_{33} E_0}{\sqrt{x_1^2 - a_0^2}} \quad \text{for } |x_1| > a_0, \tag{72}$$

$$u_3(x_1, 0) = \frac{\Delta_1 b_{41} + \Delta_2 b_{42} + \Delta b_{43}}{\Delta_1 b_{31} + \Delta_2 b_{32} + \Delta b_{33}} e_{33} E_0 \sqrt{a_0^2 - x_1^2} \quad \text{for } |x_1| < a_0, \tag{73}$$

$$E_3(x_1,0)=\frac{\Delta_1 b_{e1}+\Delta_2 b_{e2}+\Delta b_{e3}}{\Delta_1 b_{31}+\Delta_2 b_{32}+\Delta b_{33}}\left(\frac{x_1}{\sqrt{x_1^2-a_0^2}}-1\right)e_{33}E_0-E_0 \quad \text{for } |x_1|>a_0, \tag{74}$$

$$D_3(x_1,0)=\frac{\Delta_1 b_{51}+\Delta_2 b_{52}+\Delta b_{53}}{\Delta_1 b_{31}+\Delta_2 b_{32}+\Delta b_{33}}\left(\frac{x_1}{\sqrt{x_1^2-a_0^2}}-1\right)e_{33}E_0-\epsilon_{33}E_0 \quad \text{for } |x_1|>a_0, \tag{75}$$

and the electric potential is zero at $x_3=0$. Eqs. (72), (74) and (75) show that all of the stress field, electric field, and electric displacement have the square root singularity in front of crack tip, which are different from those with the traction free boundary conditions. The stress intensity factor and electric displacement intensity factor are

$$K_I^{\sigma}=\sqrt{\pi a_0}e_{33}E_0 \quad \text{and} \quad K_I^{D}=\frac{\Delta_1 b_{51}+\Delta_2 b_{52}+\Delta b_{53}}{\Delta_1 b_{31}+\Delta_2 b_{32}+\Delta b_{33}}\sqrt{\pi a_0}e_{33}E_0. \tag{76}$$

5. Energy release rate

The energy release rate for Mode I crack propagation can be obtained by calculating the energy released in closing the crack tip over an infinitesimal distance Δx_1. Considering the extension and closure of the crack increment CC' as shown in Fig. 2. The strain energy released during the closure $C'\to C$ is

$$\delta U_{\text{mech}}=2\int_{a_0+\delta x_1}^{a_0}\frac{1}{2}\sigma_{33}u_3\mathrm{d}x_1, \tag{77}$$

where the stress σ_{33} is that across CC' prior to extension; the displacement u_3 is that across CC' prior to closure.

The electrostatic energy released to close crack from C' to C is

$$\delta U_{\text{elect}}=\int_{a_0+\delta x_1}^{a_0}\frac{1}{2}\phi(x_1,0^+)D_3\mathrm{d}x_1-\int_{a_0+\delta x_1}^{a_0}\frac{1}{2}\phi(x_1,0^-)D_3\mathrm{d}x_1=-2E^a\int_{a_0+\delta x_1}^{a_0}\frac{1}{2}D_3u_3\mathrm{d}x_1, \tag{78}$$

where the electric displacement D_3 is that across CC' prior to extension. The energy release rate is given by

$$G=-\lim_{\delta x_1\to 0}\frac{\delta(U_{\text{mech}}+U_{\text{elect}})}{\delta x_1}\bigg|_{\text{constant disp.}}=\lim_{\delta x_1\to 0}\frac{1}{\delta x_1}\int_{a_0}^{a_0+\delta x_1}(\sigma_{33}-E^aD_3)u_3\mathrm{d}x_1. \tag{79}$$

Using the field distribution in front of the crack tip, the energy release rate is

$$G=\sqrt{\pi}\left(K_I^{\sigma}-E^aK_I^{D}\right)\lim_{x_1\to a_0^-}\frac{u_3(x_1,0)}{\sqrt{2(a_0-x_1)}}. \tag{80}$$

Both electric field inside the crack and electric displacement in front of the crack contribute to the energy release rate for Mode I crack propagation in linear piezoelectric materials.

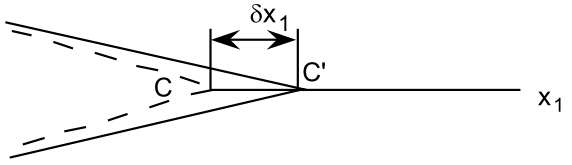

Fig. 2. Opening and closure of crack.

For mechanical loading applied onto the crack faces in the absence of electric field, consider two important cases: (1) a uniform mechanical loading applied onto the crack faces, and (2) a point loading applied in the middle of the crack faces. For a uniform mechanical loading, $\sigma_{33}(x_1,0) = -\sigma_0$, there is

$$G = \pi a_0 \sigma_0^2 \left(1 + \frac{\sigma_0}{\epsilon_0}\left[\frac{\Delta_1 b_{51} + \Delta_2 b_{52} + \Delta b_{53}}{\Delta_1 b_{31} + \Delta_2 b_{32} + \Delta b_{33}}\right]^2\right) \frac{\Delta_1 b_{41} + \Delta_2 b_{42} + \Delta b_{43}}{\Delta_1 b_{31} + \Delta_2 b_{32} + \Delta b_{33}}. \tag{81}$$

For a point force applied in the middle of the crack $\sigma_{33}(x_1,0) = -\sigma_0\delta(x_1,0)$, energy release rate is

$$G = a_0 \sigma_0^2 \frac{\sqrt{2}}{\pi} \frac{\Delta_1 b_{41} + \Delta_2 b_{42} + \Delta b_{43}}{\Delta_1 b_{31} + \Delta_2 b_{32} + \Delta b_{33}}. \tag{82}$$

For a far field electric loading in the absence of mechanical loading, the energy release rate is

$$G = \pi a_0 (e_{33} E_0)^2 \left[1 + \frac{E_0}{\epsilon_0}\left(\frac{\Delta_1 b_{51} + \Delta_2 b_{52} + \Delta b_{53}}{\Delta_1 b_{31} + \Delta_2 b_{32} + \Delta b_{33}} e_{33} + \epsilon_{33}\right) \frac{\Delta_1 b_{51} + \Delta_2 b_{52} + \Delta b_{53}}{\Delta_1 b_{31} + \Delta_2 b_{32} + \Delta b_{33}}\right] \times \frac{\Delta_1 b_{41} + \Delta_2 b_{42} + \Delta b_{43}}{\Delta_1 b_{31} + \Delta_2 b_{32} + \Delta b_{33}}. \tag{83}$$

Eqs. (81) and (83) indicate that the crack driving force for Mode I crack propagation is the third power function of uniform external loading, which is from the contribution of electrostatic energy required to propagate the crack. While the crack driving force is only proportional to the square of the external loading for a point loading applied to the crack faces, because electric field inside the crack is zero at the crack tip.

As an example, consider PZT-4 piezoelectric ceramics. The poling direction is assumed to be parallel to the x_3-axis. Its material properties are listed in Table 1 (Park and Sun, 1995). where N is the force in Newtons, C is the charge in Coulombs, V is the electric voltage in volts, and m is the length in meter. The eigenvalues of the eigenequation (20) are

$$\lambda_{1,2} = \pm 1.19103, \qquad \lambda_{3,4} = -1.08707 \pm 0.27439\mathrm{i}, \qquad \lambda_{5,6} = 1.08707 \pm 0.27439\mathrm{i}.$$

It is clear that case (d) of Eq. (28) does exist for piezoelectric materials. As shown in Fig. 3, the stress distribution in front of the crack tip has the square root singularity, which is similar to the crack-tip behavior of Mode I crack in linear fracture mechanics. Fig. 4 displays the normal stress distribution along the y-axis, which decreases with the distance from the crack face. The distribution of electric potential along the y-axis is plotted in Fig. 5. It is interesting that electric potential first increases with the distance, reaches

Table 1
Materials properties of PZT-4 piezoelectric ceramics

Elastic constants (10^{10} N/m^2)	
c_{11}	13.9
c_{12}	7.78
c_{13}	7.43
c_{33}	11.3
c_{44}	2.56
Piezoelectric constants (C/m^2)	
e_{31}	–6.98
e_{33}	13.84
e_{15}	13.44
Dielectric permittivities (10^{-9} C/Vm)	
$\in_{11}$	6.00
$\in_{33}$	5.47

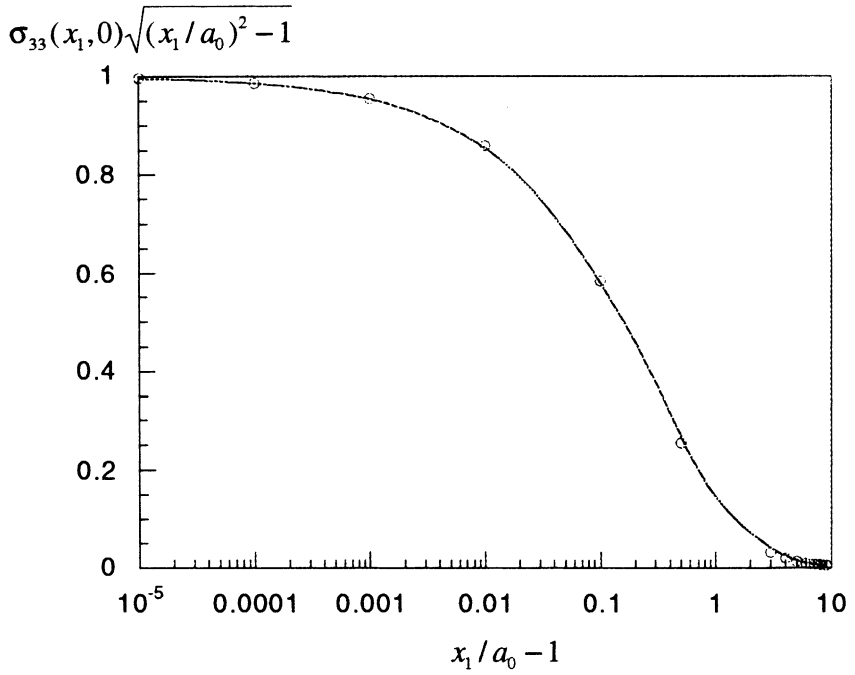

Fig. 3. Stress distribution in front of the crack tip under opening mode loading without externally applied electric field.

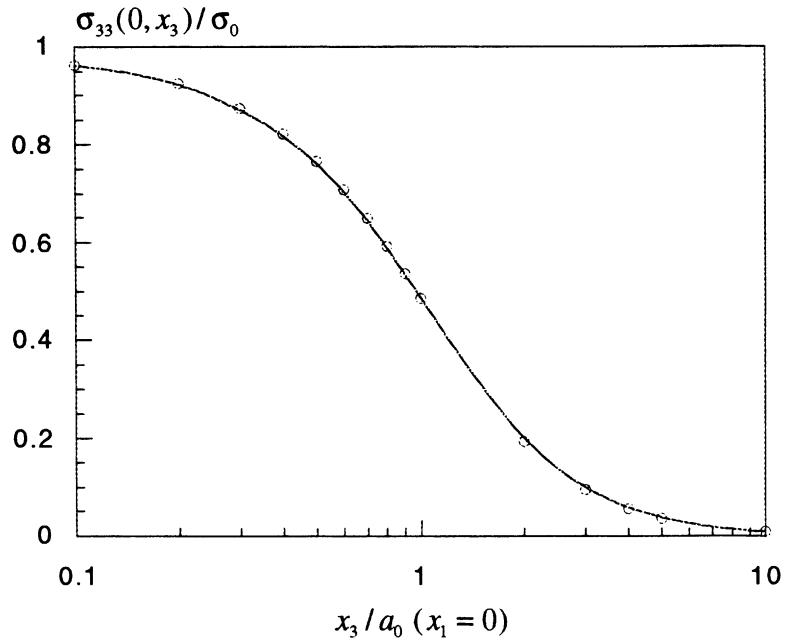

Fig. 4. Stress distribution along the *y*-axis under opening mode loading without externally applied electric field.

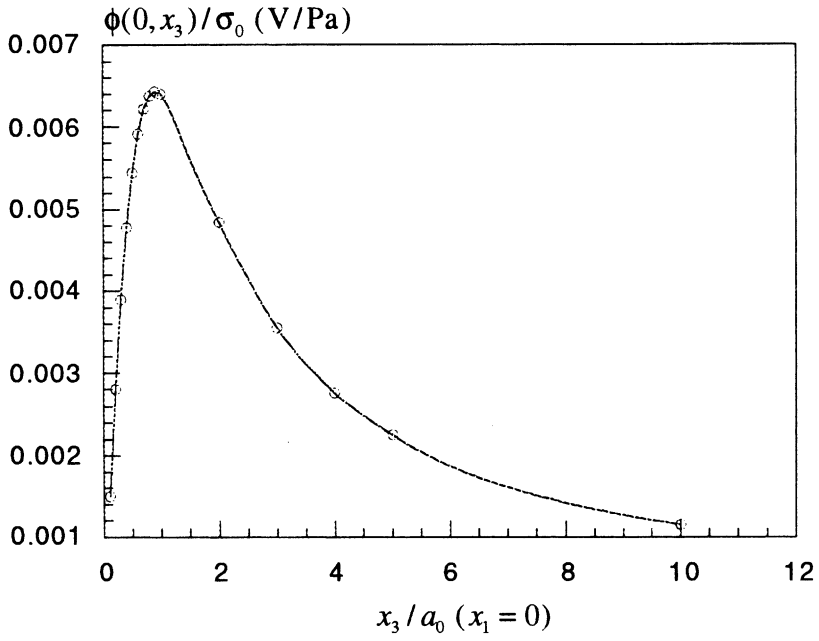

Fig. 5. Deformation induced electric field along the y-axis under opening mode loading.

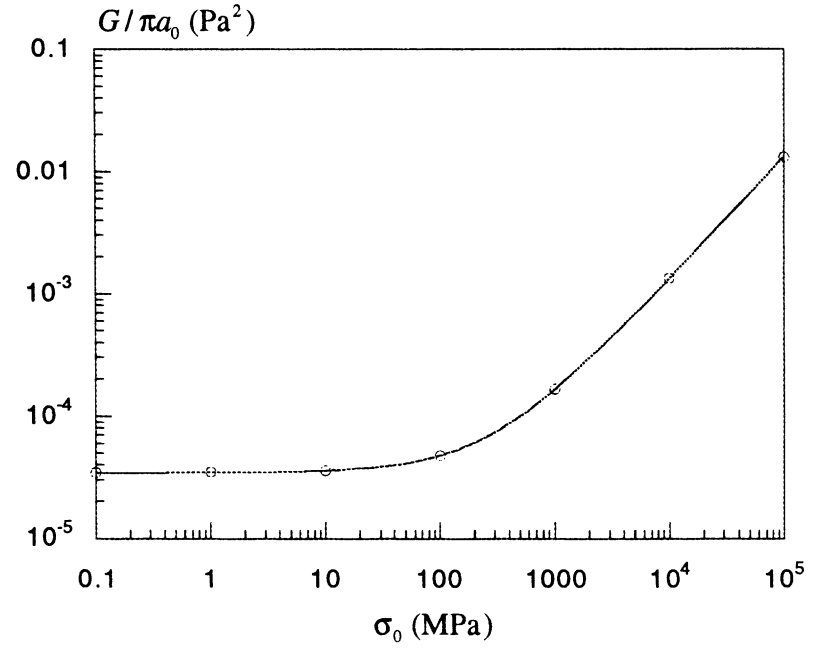

Fig. 6. Nonlinear behavior of crack driving force.

the maximum, and then decreases. The strongest electromechanical interaction along the y-axis is not at the crack faces.

Fig. 6 shows the crack driving force as a function of a uniform mechanical loading applied to the crack face. For load less than 100 MPa, the crack driving force can be approximated as proportional to the square of the mechanical load similar to linear fracture mechanics. Further increase of the load will increase the effect of the electromechanical interaction on the crack driving force and lead to the third power dependence of the crack driving force on the external load.

6. Conclusion

The electromechanical problem of a crack in an infinite piezoelectric material under electric and tension loading was studied by using the appropriate electrical boundaries on the crack faces. Four general solutions for a transversely isotropic piezoelectric material of the hexagonal crystal class 6mm have been obtained. Closed form solution of the electric potential, electric displacement field, displacement field, and stress field were obtained by using the Fourier transformation. Stress and electric field singularities were found in front of crack tip, which is similar to linear fracture mechanics. The electric field inside the crack turns out to be proportional to the mechanical loading if there is no electric loading. By including the contribution of the electrostatic energy inside the crack in the calculation of crack driving force in Mode I crack, it was found that the crack extension force is the third power function of the external loading if the electric field inside crack is not zero at crack tip. This is a nonlinear phenomenon, which was not addressed before.

Appendix A

Based on the solution of the auxiliary function f, the displacement, stresses, electric, and potential field on the upper plane are easily calculated by using Mathematica and substituting Eqs. (25)–(28) into Eqs. (14) and (16). Here, we give only the field functions for $\lambda_1^2 \neq \lambda_2^2 \neq \lambda_3^2 > 0$:

$$u_1 = \frac{2}{\pi}\sum_{i=1}^{3}\lambda_i\left(-\alpha_1+\alpha_2\lambda_i^2\right)\int_0^\infty \beta_i\xi^4\sin(\xi x_1)\mathrm{e}^{-\lambda_i\xi x_3}\mathrm{d}\xi, \tag{A.1}$$

$$u_3 = -\frac{2}{\pi}\sum_{i=1}^{3}\left(c_{11}\epsilon_{11}-\alpha_3\lambda_i^2+c_{44}\epsilon_{33}\lambda_i^4\right)\int_0^\infty \beta_i\xi^4\cos(\xi x_1)\mathrm{e}^{-\lambda_i\xi x_3}\mathrm{d}\xi, \tag{A.2}$$

$$\phi = -\frac{2}{\pi}\sum_{i=1}^{3}\left(c_{11}e_{15}-\alpha_4\lambda_i^2+c_{44}e_{33}\lambda_i^4\right)\int_0^\infty \beta_i\xi^4\cos(\xi x_1)\mathrm{e}^{-\lambda_i\xi x_3}\mathrm{d}\xi, \tag{A.3}$$

$$E_1 = -\frac{2}{\pi}\sum_{i=1}^{3}\left(c_{11}e_{15}-\alpha_4\lambda_i^2+c_{44}e_{33}\lambda_i^4\right)\int_0^\infty \beta_i\xi^5\sin(\xi x_1)\mathrm{e}^{-\lambda_i\xi x_3}\mathrm{d}\xi, \tag{A.4}$$

$$E_3 = -\frac{2}{\pi}\sum_{i=1}^{3}\lambda_i\left(c_{11}e_{15}-\alpha_4\lambda_i^2+c_{44}e_{33}\lambda_i^4\right)\int_0^\infty \beta_i\xi^5\cos(\xi x_1)\mathrm{e}^{-\lambda_i\xi x_3}\mathrm{d}\xi, \tag{A.5}$$

$$\begin{aligned}\sigma_{11} = \frac{2}{\pi}\sum_{i=1}^{3}\lambda_i\big[&c_{11}\left(-\alpha_1+\alpha_2\lambda_i^2\right)+c_{13}\left(c_{11}\epsilon_{15}-\alpha_3\lambda_i^2+c_{44}\epsilon_{33}\lambda_i^4\right)\\ &+e_{31}\left(c_{11}e_{15}-\alpha_4\lambda_i^2+c_{44}e_{33}\lambda_i^4\right)\big]\int_0^\infty \beta_i\xi^5\cos(\xi x_1)\mathrm{e}^{-\lambda_i\xi x_3}\mathrm{d}\xi,\end{aligned} \tag{A.6}$$

$$\sigma_{33} = \frac{2}{\pi}\sum_{i=1}^{3}\lambda_i\left[c_{13}\left(-\alpha_1+\alpha_2\lambda_i^2\right)+c_{33}\left(c_{11}\epsilon_{15}-\alpha_3\lambda_i^2+c_{44}\epsilon_{33}\lambda_i^4\right)\right.$$
$$\left.+\,e_{33}\left(c_{11}e_{15}-\alpha_4\lambda_i^2+c_{44}e_{33}\lambda_i^4\right)\right]\int_0^\infty \beta_i\xi^5\cos(\xi x_1)\mathrm{e}^{-\lambda_i\xi x_3}\mathrm{d}\xi, \tag{A.7}$$

$$\sigma_{13} = \frac{2}{\pi}\sum_{i=1}^{3}\left[c_{44}\lambda_i^2\left(\alpha_1-\alpha_2\lambda_i^2\right)+c_{44}\left(c_{11}\epsilon_{11}-\alpha_3\lambda_i^2+c_{44}\epsilon_{33}\lambda_i^4\right)\right.$$
$$\left.+\,e_{15}\left(c_{11}e_{15}-\alpha_4\lambda_i^2+c_{44}e_{33}\lambda_i^4\right)\right]\int_0^\infty \beta_i\xi^5\sin(\xi x_1)\mathrm{e}^{-\lambda_i\xi x_3}\mathrm{d}\xi. \tag{A.8}$$

Appendix B

Based on the solution of the auxiliary function f, constants b_{ij} are obtained from Apendix A by setting $x_3 = 0$. Here, only the constants b_{ij} for $\lambda_1^2 \neq \lambda_2^2 \neq \lambda_3^2 > 0$ are given as follows:

$$b_{1j} = c_{44}\lambda_j^2\left(\alpha_1-\alpha_2\lambda_j^2\right)+c_{44}\left(c_{11}\epsilon_{11}-\alpha_3\lambda_j^2+c_{44}\epsilon_{33}\lambda_j^4\right)+e_{15}\left(c_{11}e_{15}-\alpha_4\lambda_j^2+c_{44}e_{33}\lambda_j^4\right), \tag{B.1}$$

$$b_{2j} = -c_{11}e_{15}+\alpha_4\lambda_j^2-c_{44}e_{33}\lambda_j^4, \tag{B.2}$$

$$b_{3j} = c_{13}\lambda_j\left(-\alpha_1+\alpha_2\lambda_j^2\right)+c_{33}\lambda_j\left(c_{11}\epsilon_{11}-\alpha_3\lambda_j^2+c_{44}\epsilon_{33}\lambda_j^4\right)+\lambda_j e_{33}\left(c_{11}e_{15}-\alpha_4\lambda_j^2+c_{44}e_{33}\lambda_j^4\right), \tag{B.3}$$

$$b_{4j} = c_{11}\epsilon_{11}-\alpha_3\lambda_j^2+c_{44}\epsilon_{33}\lambda_j^4, \tag{B.4}$$

$$b_{5j} = \lambda_j\left[e_{31}\left(-\alpha_1+\alpha_2\lambda_i^2\right)+e_{33}\left(c_{11}\epsilon_{11}-\alpha_3\lambda_j^2+c_{44}\epsilon_{33}\lambda_j^4\right)-\epsilon_{33}\left(c_{11}e_{15}-\alpha_4\lambda_j^2+c_{44}e_{33}\lambda_j^4\right)\right]. \tag{B.5}$$

References

Cao, H.C., Evans, A.G., 1994. Electric field induced fatigue crack growth in piezoelectric ceramics. J. Am. Ceram. Soc. 77, 1783–1786.

Chung, H.T., Shin, B.C., Kim, H.G., 1989. Grain-size dependence of electrically induced microcracking in ferroelectric ceramics. J. Am. Ceram. Soc. 72, 327–333.

Deeg, W.F., 1980. The analysis of dislocation, crack and inclusion problems in piezoelectric solids, Ph.D. Thesis, Stanford University.

Ding, H., Chen, B., Liang, J., 1996. General solutions for coupled equations for piezoelectric medis. Int. J. Solids Struct. 33, 2283–2298.

Dunn, M.L., 1994. The effects of crack face boundary conditions on the fracture mechanics of piezoelectric solids. Engng. Fract. Mech. 48, 25–39.

Gao, H., Zhang, T.Y., Tong, P., 1997. Local and global energy release rates for an electrically yielded crack in a piezoelectric ceramic. J. Mech. Phys. Solids 45, 491–510.

Hao, T.H., Gong, X., Suo, Z., 1996. Fracture mechanics for the design of ceramic multilayer actuators. J. Mech. Phys. Solids 44, 23–48.

Jona, F., Shirane, G., 1993. Ferroelectric Crystals. Dover, New York.

Kumar, S., Singh, R.N., 1995. Crack propagation in piezoelectric materials under combined mechanical and electric loadings. Acta Mater. 44, 173–200.

Kuo, C.M., Barnett, D.M., 1991. Modern theory of anisotropic elasticity and applications. In: Wu, J.J., Ting, T.C.T., Barnett D.M. (Eds.), SIAM Proc. Ser., Philadelphia, PA, pp. 33–50.

Li, S., Cao, W., Cross, L.E., 1990. Stress and electric displacement distribution near Griffith's type III crack tips in piezoceramics. Mater. Lett. 10, 219–222.

Lynch, C.S., Yang, W., Collier, L., Suo, Z., McMeeking, R.M., 1995. Electric field induced cracking in ferroelectric ceramics. Ferroelectrics 166, 11–30.

Makino, H., Kmiya, H., 1994. Effects of DC electric field on mechanical properties of piezoelectric ceramics. Jpn. J. Appl. Phys. 33, 5323–5327.

Mason, W.P., 1950. Piezoelectric Crystals and their Application to Ultrasonics. Van Nostrand, New York.

Pak, Y.E., 1990. Crack extension force in a piezoelectric material. J. Appl. Mech. 57, 647–653.

Pak, Y.E., Tobin, A., 1993. On electric fields in fracture of piezoelectric materials. Mech. Electromag. Mater. Struct. AMD161/MD42, 51–62.

Park, S., Sun, C.T., 1995. Fracture criteria for piezoelectric ceramics. J. Am. Ceram. Soc. 78, 1475–1480.

Parton, V.Z., 1976. Fracture mechanics of piezoelectric materials. Acta Astronaut 3, 671–683.

Shindo, Y., Ozawa, E., Nowack, J.P., 1990. Singular stress and electric fields of a cracked piezoelectric strip. Appl. Electromag. Mater. 1, 77–87.

Sneddon, I.N., 1951. Fourier Transforms. McGraw-Hill, New York.

Sosa, H.A., Pak, Y.E., 1990. Three-dimensional eigenfunction analysis of a crack in a piezoelectric material. Int. J. Solids Struct. 26, 1–15.

Suo, Z., Kuo, C.M., Barnett, D.M., Willis, J.R., 1992. Fracture mechanics for piezoelectric ceramics. J. Mech. Phys. Solids 40, 739–765.

Winzer, S.R., Shanker, N., Ritter, A.P., 1989. Desiging cofired multilayer electrostrictive actuators fro reliability. J. Am. Ceram. Soc. 72, 2246–2257.

Yang, Fuqian, Kao, I., 1999. Crack problem in piezoelectric materials: general antiplane mechanical loading. Mech. Mater. 31, 395–406.

Yang, W., Suo, Z., 1994. Cracking in ceramic actuators caused by electrostriction. J. Mech. Phys. Solids 42, 649–663.

Zhang, T.Y., Hack, J.E., 1992. Mode III cracks in piezoelectric materials. J. Appl. Phys. 71, 5865–5870.

Zhang, T.Y., Tong, P., 1996. Fracture mechanics for Mode-III crack in a piezoelectric materials. Int. J. Solids Struct. 33, 343–359.

Zhang, T.Y., 1994. Effect of sample width on the energy release rate and electric boundary conditions along crack surface in piezoelectric materials. Int. J. Fract. 66, R33–R38.